

# Hypertension

JOURNAL OF THE AMERICAN HEART ASSOCIATION



*Learn and Live*<sup>SM</sup>

## **Vascular NADH/NADPH Oxidase Is Involved in Enhanced Superoxide Production in Spontaneously Hypertensive Rats**

Guillermo Zalba, Francisco J. Beaumont, Gorka San José, Ana Fortuño, María A. Fortuño, Juan C. Etayo and Javier Díez

*Hypertension* 2000;35;1055-1061

Hypertension is published by the American Heart Association, 7272 Greenville Avenue, Dallas, TX 75214

Copyright © 2000 American Heart Association. All rights reserved. Print ISSN: 0194-911X. Online ISSN: 1524-4563

The online version of this article, along with updated information and services, is located on the World Wide Web at:

<http://hyper.ahajournals.org/cgi/content/full/35/5/1055>

Subscriptions: Information about subscribing to Hypertension is online at  
<http://hyper.ahajournals.org/subscriptions/>

Permissions: Permissions & Rights Desk, Lippincott Williams & Wilkins, a division of Wolters Kluwer Health, 351 West Camden Street, Baltimore, MD 21202-2436. Phone: 410-528-4050. Fax: 410-528-8550. E-mail:  
[journalpermissions@lww.com](mailto:journalpermissions@lww.com)

Reprints: Information about reprints can be found online at  
<http://www.lww.com/reprints>

# Vascular NADH/NADPH Oxidase Is Involved in Enhanced Superoxide Production in Spontaneously Hypertensive Rats

Guillermo Zalba, Francisco J. Beaumont, Gorka San José, Ana Fortuño, María A. Fortuño, Juan C. Etayo, Javier Díez

**Abstract**—This study was designed to test the hypothesis that stimulation of nicotinamide adenine dinucleotide/nicotinamide adenine dinucleotide phosphate (NADH/NADPH) oxidase is involved in increased vascular superoxide anion ( $\cdot\text{O}_2^-$ ) production in spontaneously hypertensive rats (SHR). The study was performed in 16-week-old and 30-week-old normotensive Wistar-Kyoto rats (WKY<sub>16</sub> and WKY<sub>30</sub>, respectively) and in 16-week-old and 30-week-old SHR (SHR<sub>16</sub> and SHR<sub>30</sub>, respectively). In addition, 16-week-old SHR were treated with oral irbesartan (average dose 20 mg/kg per day) for 14 weeks (SHR<sub>30</sub>-I). Aortic NADH/NADPH oxidase activity was determined by use of chemiluminescence with lucigenin. The expression of *p22phox* messenger RNA was assessed by competitive reverse transcription–polymerase chain reaction. Vascular responses to acetylcholine were determined by isometric tension studies. Aortic wall structure was studied, determining the media thickness and the cross-sectional area by morphometric analysis. Whereas systolic blood pressure was significantly increased in the 2 groups of hypertensive animals compared with their normotensive controls, no differences were observed in systolic blood pressure between SHR<sub>30</sub> and SHR<sub>16</sub>. No other differences in the parameters measured were found between WKY<sub>16</sub> and SHR<sub>16</sub>. In SHR<sub>30</sub> compared with WKY<sub>30</sub>, we found significantly greater *p22phox* mRNA level, NADH/NADPH-driven  $\cdot\text{O}_2^-$  production, media thickness, and cross-sectional area and an impaired vasodilation in response to acetylcholine. Treated SHR had similar NADH/NADPH oxidase activity and *p22phox* expression as the WKY<sub>30</sub> group. The vascular functional and morphological parameters were improved in SHR<sub>30</sub>-I. These findings suggest that an association exists between *p22phox* gene overexpression and NADH/NADPH overactivity in the aortas of adult SHR. Enhanced NADH/NADPH oxidase–dependent  $\cdot\text{O}_2^-$  production may contribute to endothelial dysfunction and vascular hypertrophy in this genetic model of hypertension. (*Hypertension*. 2000;35:1055-1061.)

**Key Words:** endothelium ■ rats, inbred SHR ■ superoxides ■ hypertrophy

An exaggerated production of superoxide anion ( $\cdot\text{O}_2^-$ ) by the vascular wall has been observed in different animal models of hypertension, including spontaneously hypertensive rats (SHR).<sup>1–3</sup> In the majority of cases, the source of  $\cdot\text{O}_2^-$  is uncertain, although involvement of endothelial nitric oxide synthase<sup>4,5</sup> and xanthine oxidase<sup>6,7</sup> have been suggested. A growing amount of evidence supports the possibility that increased oxidative inactivation of nitric oxide (NO) by an excess of  $\cdot\text{O}_2^-$  may account for the decrease in available NO and endothelial dysfunction seen in SHR.<sup>8–10</sup> On the other hand, recent findings suggest that  $\cdot\text{O}_2^-$  may participate in vascular hypertrophy by stimulating the growth of vascular smooth muscle cells (VSMCs).<sup>11,12</sup>

Several observations suggest that the nicotinamide adenine dinucleotide/nicotinamide adenine dinucleotide phosphate (NADH/NADPH) oxidase system accounts for the majority of  $\cdot\text{O}_2^-$  generation in the vessel wall.<sup>13,14</sup> The vascular NADH/NADPH oxidase appears to be structurally and functionally different from the neutrophil oxidase. The endothelial

and VSMC NADH/NADPH oxidases are probably not all similar. All components of the NADPH-oxidase enzyme have been found in endothelial cells.<sup>15</sup> In contrast, only *p22phox* could be identified in VSMCs and has been shown to participate in the increased  $\cdot\text{O}_2^-$  production on stimulation with angiotensin II.<sup>16</sup>

We have hypothesized that stimulation of NADH/NADPH oxidase may contribute to increased vascular  $\cdot\text{O}_2^-$  production in SHR. Thus, the present study was designed to test whether NADH/NADPH oxidase activity is enhanced and *p22phox* gene expression is upregulated in the aortas of SHR. In addition, we also investigated whether blockade of angiotensin II type 1 (AT<sub>1</sub>) receptors with irbesartan modifies the enzyme in SHR.

## Methods

### Animals and Design

The investigation was performed according to the European Community guidelines for animal ethical care and use of laboratory

Received October 11, 1999; first decision November 24, 1999; revision accepted December 16, 1999.

From the Vascular Pathophysiology Unit, School of Medicine, University of Navarra, Pamplona, Spain.

Correspondence to Javier Díez, MD, PhD, Unidad de Fisiopatología Vascular, Facultad de Medicina, C/Irunlarrea s/n, 31080 Pamplona, Spain. E-mail jadimar@unav.es

© 2000 American Heart Association, Inc.

*Hypertension* is available at <http://www.hypertensionaha.org>

animals (Directive 86/609). Experiments were performed with rats provided by Harlan UK Limited (Blackthorn, Bicester, Oxon, UK). The rats were housed in cages maintained in a humidity- and temperature-controlled room and fed a standard diet. Sixteen-week-old male SHR (n=90) and their normotensive genetic controls, Wistar-Kyoto rats (WKY) (n=60), were studied in the following manner: (1) 16-week-old WKY (n=30) and SHR (n=30) were killed to perform studies in young rats (groups WKY<sub>16</sub> and SHR<sub>16</sub>, respectively); (2) 16-week-old WKY (n=30) and SHR (n=30) were observed in our colony for additional 14 weeks and killed at 30 weeks of age to perform studies in adult rats (groups WKY<sub>30</sub> and SHR<sub>30</sub>, respectively), and (3) 16-week-old SHR (n=30) were treated with irbesartan and killed at 30 weeks. The drug was dissolved in drinking water and the concentration was adjusted for the daily water intake and body weight to obtain an average daily dose of 20 mg/kg body wt. In each group of animals, 10 rats were used to measure endothelial function in intact vessels and NADH/NADPH oxidase activity in vessel homogenates, 10 rats were used to determine vascular *p22phox* messenger RNA (mRNA) expression, and the remaining 10 rats were used for aortic morphometric analysis.

Systolic blood pressure (SBP) was measured every 2 weeks by the standard tail-cuff method. For measurement of isometric wall tension and enzymatic and molecular studies, rats were killed by decapitation. The thoracic aorta then was carefully excised and dissected, adventitial tissues were carefully removed, and the vascular wall was washed thoroughly with normal saline to remove any contaminating blood.

### Measurement of $\cdot\text{O}_2^-$ Production in Aortic Homogenates

Vascular  $\cdot\text{O}_2^-$  was estimated with lucigenin-enhanced chemiluminescence.<sup>17</sup> Aortic segments (2 to 3 cm) were placed in chilled modified Krebs/HEPES buffer and homogenized on ice with a glass/glass motor-driven tissue homogenizer for 2 minutes in 50 mmol/L PBS, which contained 0.01 mmol/L EDTA. In some experiments the endothelium was removed by rubbing. The homogenate was centrifuged at 1000g for 10 minutes. The pellet was discarded and the supernatant was stored on ice until use. Protein content was measured by the method of Bradford.<sup>18</sup> NADH or NADPH oxidase activity was measured by chemiluminescence in a scintillation vial containing HEPES buffer, 250  $\mu\text{mol/L}$  lucigenin, in 2 mL buffer phosphate. The chemiluminescence, which occurred over the ensuing 5 minutes in response to the addition of either 100  $\mu\text{mol/L}$  NADH or 100  $\mu\text{mol/L}$  NADPH, was recorded. No activity could be measured in the absence of NADH or NADPH. Reactions were initiated by the addition of 20  $\mu\text{L}$  homogenate. To determine the  $\cdot\text{O}_2^-$  dependency of the lucigenin-enhanced chemiluminescence obtained from vascular homogenates, we examined the effect of  $\text{Cu}^{2+}/\text{Zn}^{2+}$  superoxide dismutase (SOD) (2000 U/mL) on  $\cdot\text{O}_2^-$  production after stimulation of homogenates with NADH. In some experiments, membranes and cytosol were separated by centrifugation (50 000g for 30 minutes). Twenty-five microliters of either the supernatant or the particulate fraction were used to examine NADH oxidase-dependent and NADPH oxidase-dependent  $\cdot\text{O}_2^-$  production of these subcellular fractions.

### Endothelium-Dependent and Endothelium-Independent Relaxations

After washing, each aorta was cut into 2- to 3-mm rings (6 per rat). The rings were suspended in a vessel that contained 10 mL of Krebs-Henseleit solution with the following composition (in mmol/L): 118.4 NaCl, 4.74 KCl, 1.18  $\text{MgSO}_4$ , 0.7  $\text{H}_2\text{O}$ , 1.19  $\text{KH}_2\text{PO}_4$ , 2.52  $\text{CaCl}_2$ , 0.2  $\text{H}_2\text{O}$ , 25  $\text{NaHCO}_3$ , and 11.5 glucose (pH, 7.34). The solution was oxygenated with a 95%  $\text{O}_2$ -5%  $\text{CO}_2$  mixture and maintained at 37°C in a thermostated bath. Two stainless steel wires were inserted into the vascular lumen; one was anchored to a stationary support and the other was connected to a force isometric transducer. The rings were incubated for 60 minutes for equilibration at a resting tension of 2g with buffer exchanges every 15 minutes during this period. Changes in isometric forces were analyzed and

recorded by an Isolated Organs Data Acquisition Program (Proto5). The rings were then maximally contracted with norepinephrine ( $10^{-7}$  mol/L), and once a plateau had been reached, the endothelium-dependent and endothelium-independent relaxations were studied by plotting the concentration-response curves for the responses to  $10^{-9}$  to  $10^{-5}$  mol/L acetylcholine (ACh) and to  $10^{-9}$  to  $10^{-6}$  mol/L sodium nitroprusside (SNP), respectively. Endothelium-dependent and endothelium-independent relaxations were expressed as percentages of decline of the contraction induced by norepinephrine. These values were then plotted against the negative logarithm of the agonist dose to produce dose-response curves. Dose-response curves were analyzed, and the  $\text{EC}_{50}$  value (the concentration for half-maximal response) for relaxation of each ring was calculated by logistic analysis and expressed as the  $\text{pD}_2$  defined as  $-\log(\text{EC}_{50})$ .

### Reverse Transcription-Polymerase Chain Reaction for *p22phox*

Total RNA was extracted from homogenized thoracic aortas with the use of Ultraspec RNA reagent. mRNA was isolated from total RNA with the Oligotex mRNA kit (Qiagen), and mRNA concentration was determined spectrometrically. The expression of *p22phox* was quantified in the aorta by a competitive reverse transcription-polymerase chain reaction (RT-PCR) method, as described by Gilliland et al.<sup>19</sup> On the basis of rat *p22phox* cDNA sequence,<sup>20</sup> the oligonucleotides 5'-GCTCATCTGTCTGCTGGAGTA-3' and 5'-ACGACCTCATCTGTCCTGGA-3' were selected as sense and antisense primers, respectively. The *p22phox*-specific primers amplified a 435-bp PCR product. The identity of this PCR product was verified by sequencing. The heterologous DNA template (*p22phox* competitor) was constructed with the use of a PCR-MIMIC construction kit (Clontech), following the manufacturer's instructions. The obtained 318-bp *p22phox* competitor contained the *p22phox* gene-specific sequences incorporated at the ends. This 318-bp fragment was cloned in a pGEMT vector (Promega), linearized by digestion with *Sca I*, and subjected to in vitro transcription into RNA. The purified *p22phox*-construct RNA was quantified spectrometrically.

Both RT and PCR were performed in a single tube with gene-specific primers and specific target RNAs, with the use of the Superscript 1-step RT-PCR System (Life Technologies). RT-PCR was performed with constant amounts of aortic mRNA (35 ng) together with a range of amounts between  $10^6$  and  $10^5$  molecules of competitor RNA. RT-PCR reaction mixture (50  $\mu\text{L}$ ) contained aortic and competitor RNA, a buffer containing 0.2 mmol/L of each dNTP, and 1.2 mmol/L  $\text{MgSO}_4$ , 20 pmol/L of primer, 20 U of Rnase inhibitor (Pharmacia Biotech Inc), and 1  $\mu\text{L}$  of a RT/Taq Mix containing a mixture of Superscript II Reverse Transcriptase and Taq DNA Polymerase. All components necessary for RT-PCR were mixed in 1 tube, and RT (55°C for 30 minutes and then to 94°C for 2 minutes) was automatically followed by PCR cycling (35 cycles with a temperature profile of 94°C for 20 seconds, 60°C for 25 seconds, and 72°C for 1 minute and finally 5 minutes at 72°C for quantification of *p22phox* mRNA) without additional steps. The PCR products were run on a 2% agarose gel, stained with ethidium bromide, visualized by UV illumination, and photographed. The amounts of target and competitor PCR product were quantified by densitometric scanning of the film negative. To correct for differences in size of target (435 bp) and competitor (318 bp) *p22phox* PCR products, the amounts of competitor PCR product were multiplied by 1.368 (435/318). The ratio of target to competitor PCR product was plotted against the number of competitor construct molecules on a log-log scale. At the point in which equal molar amounts of target and competitor product were yielded by PCR (ie, competition ratio=1), the original number of transcript in the aortic sample was defined by the known input of competitor construct molecules.

### Vascular Morphology

Before the animals were killed, they were weighted and anesthetized (sodium thiopental, 30 mg/kg IP). Subsequently, the thoracic aorta was fixed by retrograde perfusion as we have previously described.<sup>21</sup>

**Blood Pressure and Parameters of Vascular Function and Morphology in Normotensive and Hypertensive Rats**

Parameter	WKY <sub>16</sub>	SHR <sub>16</sub>	WKY <sub>30</sub>	SHR <sub>30</sub>	SHR <sub>30-I</sub>
SBP, mm Hg	163±4	234±5*	164±3	230±3*	182±2
Endothelium-dependent relaxations					
Maximum response to Ach, %	80±7	66±6	80±5	34±5†	74±6
pD <sub>2</sub> (to Ach)	6.47±0.11	6.44±0.18	6.31±0.17	6.41±0.13	6.59±0.21
Endothelium-independent relaxations					
pD <sub>2</sub> (to SNP)	8.26±0.06	8.32±0.09	8.38±0.08	8.07±0.05‡	7.90±0.09‡
Media thickness, mm	0.176±0.009	0.177±0.006	0.196±0.006	0.226±0.008‡	0.207±0.010
Cross-sectional area, mm <sup>2</sup>	0.423±0.023	0.443±0.021	0.477±0.019	0.632±0.035‡	0.573±0.036

Values are expressed as mean±SEM of 10 rats.

\**P*<0.01 compared with WKY<sub>16</sub>, WKY<sub>30</sub>, and SHR<sub>30-I</sub>.

†*P*<0.05 compared with WKY<sub>16</sub>, SHR<sub>16</sub>, WKY<sub>30</sub>, and SHR<sub>30-I</sub>.

‡*P*<0.05 compared with WKY<sub>16</sub>, SHR<sub>16</sub>, and WKY<sub>30</sub>.

In brief, the aorta was cannulated with a polyethylene catheter, the heart was arrested in diastole by an intracarotid injection of KCl (1.0 mol/L, 1 mL), and the right atria were incised to allow drainage of blood and perfusate. After initial perfusion with normal saline buffer to wash the blood, 4% paraformaldehyde was perfused for 5 minutes at a pressure equal to the mean arterial pressure determined before the animals were killed. The thoracic aorta was excised and transversally cut in 8 slices. The slices were alternatively separated into 2 groups, postfixed for 5 hours by immersion in buffered 4% paraformaldehyde and 10% formalin, respectively, and finally, dehydrated and embedded in paraffin. Transversal sections (4 μm in thickness) of the thoracic aorta were obtained from the 4 paraformaldehyde-fixed, paraffin-embedded specimens. Media thickness (MT) and cross-sectional area (CSA) were determined by morphometry with an automated image analysis system (Visilog 4.1.5, Noesis) as previously described by van Gorp et al.<sup>22</sup> For this purpose, 1 section of each specimen (4 from each rat) was stained for elastin fibers. Sections were analyzed under the microscope (×4), and images of the whole aortic ring were digitized (final resolution of 85.5 mm<sup>2</sup>/pixel). Stained elastic lamellae were segmented by interactive gray-level thresholding, and after binary processing and analysis, CSA and MT were obtained. CSA reflects the degree of arterial hypertrophy better than MT because it is not influenced by the variations in the perfusion pressure.<sup>23</sup>

A monoclonal mouse antibody against rat monocyte/macrophages (ED1, Serotec)<sup>24</sup> at a concentration of 1:100 in PBS was applied for 20 minutes. In control experiments, we checked that ED1 is specific for rat monocyte macrophages and does not recognize granulocytes, lymphocytes, endothelial cells, or smooth muscle cells. Fluorescein-conjugated goat anti-mouse antibody (Dakopatts) was used as a second antibody at a concentration of 1:40.

### Statistical Analysis

Data are expressed as mean±SEM. Differences among the 5 groups of rats were tested by a 1-way ANOVA. A Scheffé's post hoc test was used to examine differences between groups when significance was indicated. Probability values <0.05 were considered significant.

## Results

### Blood Pressure

At the age of 16 weeks, SBP was higher (*P*<0.01) in SHR<sub>16</sub> than in WKY<sub>16</sub> (Table). Values of SBP remained higher in SHR than in WKY along the experimental 14-week period. Therefore, at the end of the 14-week-period of observation, SBP was higher (*P*<0.01) in SHR<sub>30</sub> than in WKY<sub>30</sub> (Table). No differences were found in SBP between SHR<sub>30</sub> and SHR<sub>16</sub>. SBP was lower (*P*<0.01) in SHR<sub>30-I</sub> than in SHR<sub>30</sub> (Table).

Most rats (80%) in the SHR<sub>30-I</sub> group exhibited final values of SBP above the upper normal limit measured in WKY<sub>30</sub> (176 mm Hg).

### *p22phox* mRNA Expression

In preliminary experiments, we proved that there were no differences in the rate of transcription of the target and competitor sequences. A representative competitive RT-PCR experiment of aortic *p22phox* mRNA in young and adult rats is shown in Figure 1a. In initial experiments, *p22phox* was amplified from cDNA in the presence of several serial dilutions of the *p22phox* competitor. The results of these experiments enabled us to find the most appropriate amounts of the *p22phox* competitor. Thus, definitive experiments were performed with different amounts of *p22phox* competitor comprised between 10<sup>5</sup> and 10<sup>6</sup> molecules. No differences in the *p22phox* mRNA level were found between WKY<sub>16</sub> and SHR<sub>16</sub> (3685±813 versus 4218±707 molecules of *p22phox* mRNA/ng mRNA) (Figure 1b). In contrast, *p22phox* mRNA level was 2.5-fold higher in SHR<sub>30</sub> than in WKY<sub>30</sub> (10 455±1056 versus 4221±349 molecules of *p22phox* mRNA/ng mRNA, *P*<0.01) (Figure 1b). Furthermore, the *p22phox* mRNA level was greater (*P*<0.01) in SHR<sub>30</sub> than in SHR<sub>16</sub>. After treatment with irbesartan, *p22phox* mRNA expression was lower (*P*<0.01) in SHR<sub>30-I</sub> (3456 molecules of *p22phox* mRNA/ng mRNA) than in SHR<sub>30</sub>, and the values in treated SHR were similar to those measured in WKY<sub>30</sub> (Figure 1b).

### NADH/NADPH Oxidase Activity

No differences were found between WKY<sub>16</sub> and SHR<sub>16</sub> in NADH oxidase activity (5.45±0.66 versus 5.96±0.77 nmol · O<sub>2</sub><sup>-</sup> · min<sup>-1</sup> · mg<sup>-1</sup>) and NADPH oxidase activity (1.92±0.16 versus 1.73±0.27 nmol · O<sub>2</sub><sup>-</sup> · min<sup>-1</sup> · mg<sup>-1</sup>) (Figure 2). In contrast, both activities were higher (*P*<0.01) in SHR<sub>30</sub> than in WKY<sub>30</sub> (11.01±0.81 versus 5.81±0.74 nmol · O<sub>2</sub><sup>-</sup> · min<sup>-1</sup> · mg<sup>-1</sup> for NADH oxidase activity; 5.09±0.41 versus 2.21±0.19 nmol · O<sub>2</sub><sup>-</sup> · min<sup>-1</sup> · mg<sup>-1</sup> for NADPH oxidase activity). The activity of the oxidase was lower (*P*<0.01) in SHR<sub>30-I</sub> than in SHR<sub>30</sub> (5.50±0.53 nmol · O<sub>2</sub><sup>-</sup> · min<sup>-1</sup> · mg<sup>-1</sup> for NADH oxidase activity and 2.31±0.27 nmol · O<sub>2</sub><sup>-</sup> · min<sup>-1</sup> · mg<sup>-1</sup> for NADPH oxidase activity) (Figure 2).

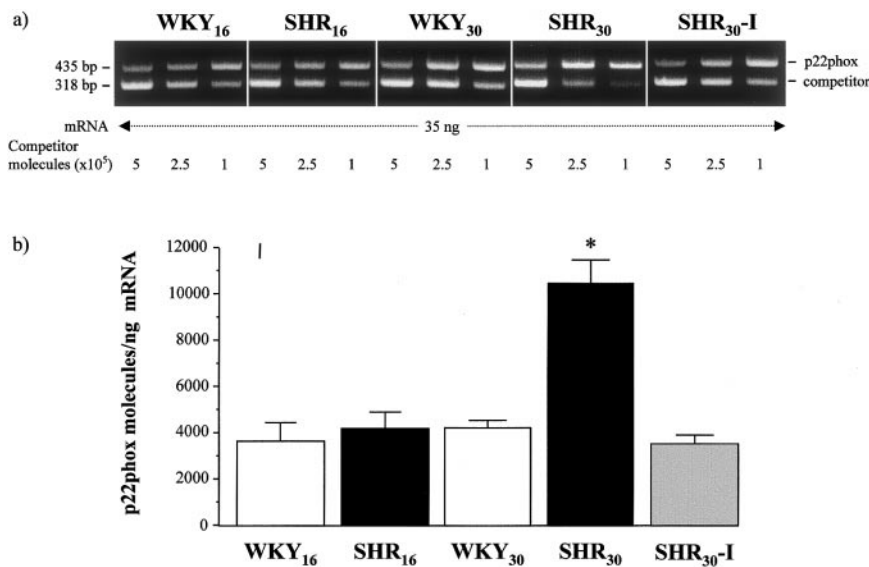


**Figure 1.** Quantification of aortic *p22phox* mRNA by competitive RT-PCR. a, Representative experiment for measurement of *p22phox* mRNA levels in aortas of WKY<sub>16</sub>, SHR<sub>16</sub>, WKY<sub>30</sub>, SHR<sub>30</sub>, and SHR<sub>30-I</sub>. As indicated at bottom of gel, constant amount of mRNA was used for competitive RT-PCR with different amounts of *p22phox*-construct RNA molecules as competitor. b, *p22phox* mRNA levels in aorta measured by competitive RT-PCR in WKY<sub>16</sub>, SHR<sub>16</sub>, WKY<sub>30</sub>, SHR<sub>30</sub>, and SHR<sub>30-I</sub>. Bars represent mean ± SEM of 10 animals in each group. \**P* < 0.01 compared with WKY<sub>16</sub>, WKY<sub>30</sub>, SHR<sub>16</sub>, and SHR<sub>30-I</sub>.

To assess the cellular source of increased NADH/NADPH oxidase activity in the vascular wall, some experiments were performed in deendothelized preparations. Although removal of the endothelium diminished slightly the NADH oxidase activity in aortic homogenates from SHR<sub>30</sub> (with endothelium, 10.57 ± 0.17 nmol · O<sub>2</sub><sup>-</sup> · min<sup>-1</sup> · mg<sup>-1</sup>; without endothelium, 8.62 ± 0.51 nmol · O<sub>2</sub><sup>-</sup> · min<sup>-1</sup> · mg<sup>-1</sup>), the difference was not statistically significant.

To determine the ·O<sub>2</sub><sup>-</sup> dependency of the lucigenin-enhanced chemiluminescence obtained from homogenates of rat aorta, we examined the effect of native Cu<sup>2+</sup>/Zn<sup>2+</sup> SOD. As shown in Figure 3, SOD at very high concentrations (2000 U/mL) was effective in reducing the chemiluminescence signal in response to stimulation with NADH.

NADH-dependent and NADPH-dependent oxidase activities in adult rats were located predominantly in the particulate fraction (Figure 4). NADH-driven ·O<sub>2</sub><sup>-</sup> production measured in the particulate fraction was higher (*P* < 0.01) in SHR<sub>30</sub> than in WKY<sub>30</sub> (159 ± 16 versus 59 ± 6 nmol · min<sup>-1</sup> · mg<sup>-1</sup>). NADPH-driven ·O<sub>2</sub><sup>-</sup> production measured in the particulate fraction was also higher (*P* < 0.01) in SHR<sub>30</sub> than in WKY<sub>30</sub> (48 ± 3.7 versus 11.9 ± 2.1 nmol · min<sup>-1</sup> · mg<sup>-1</sup>). Cytosolic activity was minimal in all the animals tested (Figure 4).

High concentrations of lucigenin can produce a redox cycle with flavin-containing enzymes, leading to artifactual increases in estimates of ·O<sub>2</sub><sup>-</sup>.<sup>25</sup> This does not occur with low

concentrations of lucigenin (5 μmol/L).<sup>26</sup> Experiments with 5 μmol/L lucigenin revealed that NADH oxidase activity was greater (*P* < 0.01) in aortas from SHR<sub>30</sub> than in aortas from WKY<sub>30</sub> (99 ± 3 vs 56 ± 3 counts · min<sup>-1</sup> · μg<sup>-1</sup>).

### Vascular Relaxations

Whereas no differences in the maximal relaxations in response to Ach were observed between WKY<sub>16</sub> and SHR<sub>16</sub>, this parameter was lower (*P* < 0.05) in SHR<sub>30</sub> than in WKY<sub>30</sub> (Table). Furthermore, the response to Ach was lower (*P* < 0.05) in SHR<sub>30</sub> than in SHR<sub>16</sub> (Table). Irbesartan-treated SHR exhibited a normal response to Ach (Table). There were no significant differences in the sensitivity to Ach (pD<sub>2</sub> values) among the different groups of animals (Table).

Maximum endothelium-independent relaxations to SNP were reached at the same concentration (3 × 10<sup>-6</sup> mol/L) in hypertensive and normotensive rats, irrespective of age and treatment. There were no significant differences in the pD<sub>2</sub> values between WKY<sub>16</sub> and SHR<sub>16</sub> (Table). Nevertheless, pD<sub>2</sub> values were lower (*P* < 0.05) in SHR<sub>30</sub> and SHR<sub>30-I</sub> than in WKY<sub>30</sub> (Table).

### Morphological Analysis

There were no differences in MT and CSA between WKY<sub>16</sub> and SHR<sub>16</sub> (Table). Otherwise, MT and CSA were greater (*P* < 0.05) in SHR<sub>30</sub> than in WKY<sub>30</sub> and SHR<sub>16</sub> (Table).

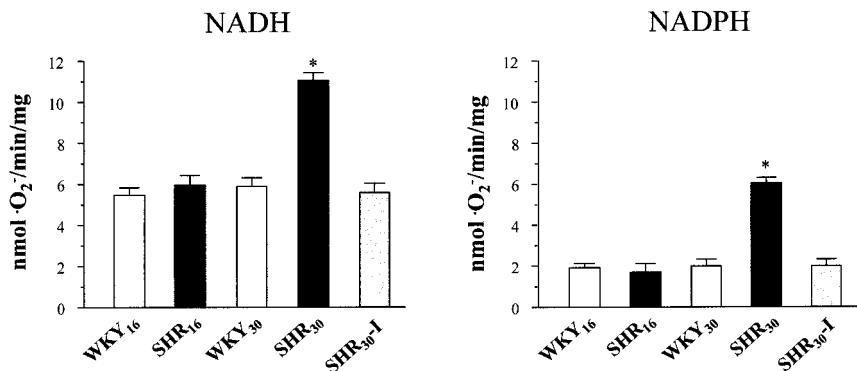


**Figure 2.** NADH-driven (left) and NADPH-driven (right) ·O<sub>2</sub><sup>-</sup> production in homogenates from aortic tissue from WKY<sub>16</sub>, SHR<sub>16</sub>, WKY<sub>30</sub>, SHR<sub>30</sub>, and SHR<sub>30-I</sub>. Bars represent mean ± SEM of 10 animals in each group. \**P* < 0.05 compared with WKY<sub>16</sub>, SHR<sub>16</sub>, WKY<sub>30</sub>, and SHR<sub>30-I</sub>.

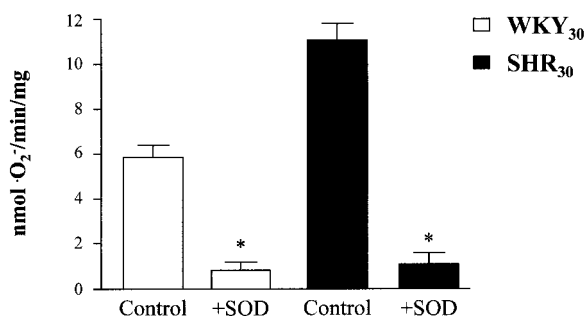


**Figure 3.** Effect of SOD on NADH-driven  $\cdot\text{O}_2^-$  production in homogenates from aortic tissue from WKY<sub>30</sub> and SHR<sub>30</sub>. Bars represent mean  $\pm$  SEM of 10 animals in each group. \* $P < 0.05$  compared with control.

Although the values of MT and CSA were lower in SHR<sub>30</sub>-I than in SHR<sub>30</sub>, the difference was not significant (Table). No differences were observed in these 2 parameters between SHR<sub>30</sub>-I and WKY<sub>30</sub> (Table).

In WKY and SHR, immunofluorescence did not reveal any ED1-positive cells in the aorta. The absence of monocyte-macrophages in SHR aorta was confirmed by light microscopy and morphological evaluation.

### Discussion

The observations of the present study provide the first indication that NADH/NADPH oxidase activity is increased in the aortic wall of adult SHR and that this overactivity is associated with upregulation of *p22phox* mRNA. In addition, we found that overactivity of NADH/NADPH oxidase was associated with impaired NO-dependent relaxation and media hypertrophy in the aortas of adult SHR. Interestingly, the enzyme abnormalities were not observed in the aortas of SHR chronically treated with the AT<sub>1</sub> receptor antagonist irbesartan.

The NADH/NADPH oxidase is expressed in endothelial cells,<sup>12</sup> VSMCs,<sup>12,16,27</sup> adventitial fibroblasts,<sup>14,28</sup> and inflammatory neutrophils.<sup>29</sup> Although we did not perform in situ hybridization to determine which cell type(s) overexpress *p22phox* mRNA, several findings support a role for VSMCs as the potential source for oxidase overactivity found in adult SHR. First, the examination of NADH/NADPH activity was

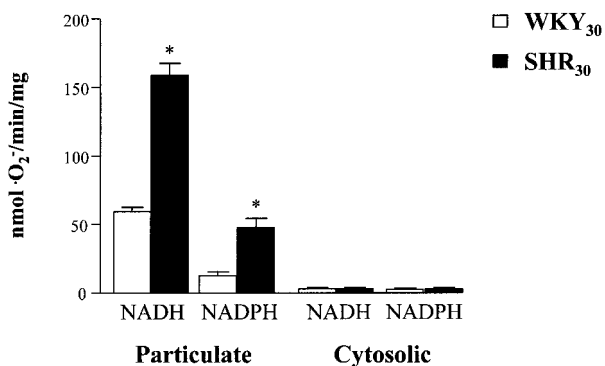


**Figure 4.** Subcellular localization of NADH oxidase and NADPH oxidase activity in vascular homogenates from WKY<sub>30</sub> and SHR<sub>30</sub>. Bars represent mean  $\pm$  SEM of 10 animals in each group. \* $P < 0.01$  compared with WKY<sub>30</sub>.

performed in aortas in which the adventitial tissue had been previously removed. Second, deendothelialization did not affect the level of NADH/NADPH oxidase activity. Third, increased NADH/NADPH oxidase activity was associated with hypertrophy of the media. Fourth, although it has been reported that in the aortas of SHR exist an augmented infiltration of monocyte-macrophage cells compared with the aortas of WKY,<sup>30</sup> we did not observe such an abnormality in the aortas of adult SHR after microscopic examination. Further, the preferred substrate for oxidases in macrophages and neutrophils is NADPH rather than NADH.<sup>27</sup>

It is unclear which factors may be involved in upregulation of *p22phox* mRNA expression present in the aortas of adult SHR. It has been reported that hydralazine decreases both blood pressure and NADPH oxidase activity in the aortas of rats with experimentally induced hypertension.<sup>31</sup> Thus, it is possible that the increase in blood pressure is the stimulus that induces *p22phox* mRNA expression in the aortas of adult SHR. However, it has been shown that norepinephrine-induced hypertension does not increase vascular NADH/NADPH oxidase activity.<sup>17</sup> The same authors have reported that infusion of low amounts of angiotensin II that do not increase blood pressure results in the increase in this oxidase activity. Moreover, we found that *p22phox* mRNA expression was normal in young SHR exhibiting the same degree of elevation in blood pressure than did adult SHR. It therefore appears that long-term exposure to arterial hypertension is necessary to induce *p22phox* overexpression in SHR aorta. Alternatively, other nonhemodynamic factors may be also involved in this alteration (ie, tissue hormones and cytokines).

One of these candidate factors is angiotensin II. As previously mentioned, it has been found that *p22phox* mRNA expression was elevated in rats receiving angiotensin II infusion.<sup>31</sup> This effect was inhibited by treatment with losartan, suggesting that it was mediated by the interaction of angiotensin II with AT<sub>1</sub> receptors at the vascular wall. In addition, angiotensin II has been found to stimulate *p22phox* expression and  $\cdot\text{O}_2^-$  production in VSMCs.<sup>16</sup> Exaggerated production of angiotensin II<sup>32</sup> and enhanced expression of both AT<sub>1</sub> receptor and angiotensin-converting enzyme<sup>33</sup> have been reported in vessels of SHR compared with WKY. Furthermore, an age-dependent increase of vascular angiotensin-converting enzyme activity in SHR has been shown.<sup>34</sup> Altogether these data would suggest that high levels of vascular angiotensin II can participate in *p22phox* overexpression in the aortas of adult SHR. This possibility is further supported by our findings that both *p22phox* mRNA expression and NADH/NADPH oxidase activity are normalized in irbesartan-treated SHR despite a noncomplete normalization of blood pressure.

It has been suggested that the development of endothelial dysfunction is linked to an exaggerated production of  $\cdot\text{O}_2^-$  in aortas from SHR.<sup>8</sup> An enhanced production of  $\cdot\text{O}_2^-$  may result in inactivation of NO and generation of peroxynitrite.<sup>35</sup> The resulting decrease in NO availability might be involved in the impairment of NO-dependent relaxations.<sup>2,3,8-10</sup> Thus, oxidative degradation of NO caused by increased  $\cdot\text{O}_2^-$  secondary to overactivity of NADH/NADPH oxidase likely

explains the diminished response to Ach observed in the aortas of adult SHR. This is further supported by the finding that responses to Ach are normal in irbesartan-treated SHR, which exhibit normal NADH/NADPH oxidase activity. Of course, our results do not exclude a role for other potential sources of  $\cdot\text{O}_2^-$  (endothelial NO synthase, xanthine oxidase) in the vascular wall of adult SHR. On the other hand, the observation that responses to SNP are altered in both untreated and treated SHR suggests that other molecular alterations (ie, diminished expression and activity of VSMC guanylate cyclase)<sup>36,37</sup> may also contribute to impaired vasodilatory responsiveness in SHR.

On the other hand, it is possible that  $\cdot\text{O}_2^-$  is also involved in vascular hypertrophy. Recently, it has been shown that  $\cdot\text{O}_2^-$  stimulates the proliferation of VSMCs.<sup>11</sup> In addition, a role for NADH/NADPH oxidase-derived  $\cdot\text{O}_2^-$  and  $\text{H}_2\text{O}_2$  has been proposed in angiotensin II-induced VSMC growth.<sup>12</sup> Therefore, the association of NADH/NADPH oxidase overactivity with medial hypertrophy in the aortas of adult SHR suggests a contributing role for the enzyme in vascular wall remodeling. The finding that the dimensions of the aortic wall were not completely normalized in irbesartan-treated SHR suggests that the maintenance of increased levels of blood pressure after treatment may also account for the persistence of a certain degree of aortic hypertrophy in these rats.

In summary, we reported that NADH/NADPH oxidase activity is abnormally increased in the aortic wall of adult SHR and that this abnormality is associated with upregulated *p22phox* mRNA expression. Our findings suggest that long-term exposure to hypertension, possibly combined with other factors (ie, local overproduction of angiotensin II), may play a role in *p22phox* upregulation and enzyme overactivity in the media layer from the aortas of these rats. Enhanced NADH/NADPH oxidase-mediated  $\cdot\text{O}_2^-$  production might contribute to functional and structural alterations present in the aortas of adult SHR. Further experiments are necessary to elucidate the precise mechanism through which chronic blockade of AT<sub>1</sub> receptors prevents overstimulation of vascular NADH/NADPH oxidase in this genetic model of hypertension. The significance of these experimental results is underlined by clinical data indicating the occurrence of increased  $\cdot\text{O}_2^-$  production in humans with essential hypertension.<sup>38,39</sup>

### Acknowledgments

This work was supported by grant CDTI 96-0035 from the Ministry of Industry and the Ministry of Education and Culture, Spain.

### References

- Bouloumie A, Bauersachs J, Linz W, Scholkens BA, Wiemer G, Fleming I, Busse R. Endothelial dysfunction coincides with an enhanced nitric oxide synthase expression and superoxide anion production. *Hypertension*. 1997;30:934–941.
- Suzuki H, Swee A, Zweifach BW, Schmid-Schonbein GW. In vivo evidence for microvascular oxidative stress in spontaneously hypertensive rats. *Hypertension*. 1995;25:1083–1089.
- Dohi Y, Theil M, Bühler FR, Lüscher TF. Activation of the endothelial L-arginine pathway in pressurized mesenteric resistance arteries: effect of age and hypertension. *Hypertension*. 1990;15:170–175.
- Cosentino F, Patton S, d'Uscio LV, Werner ER, Werner-Felmayer G, Moreau P, Malinski T, Lüscher TF. Tetrahydrobiopterin alters superoxide and nitric oxide release in prehypertensive rats. *J Clin Invest*. 1998;101:1530–1537.
- Kerr S, Brosnan MJ, McIntyre M, Reid JL, Dominiczak AF, Hamilton CA. Superoxide anion production is increased in a model of genetic hypertension: role of endothelium. *Hypertension*. 1999;33:1353–1358.
- Nakazono K, Watanabe N, Matsuno K, Sasaki J, Sato T, Inoue M. Does superoxide underlie the pathogenesis of hypertension? *Proc Natl Acad Sci U S A*. 1991;88:10045–10048.
- Miyamoto Y, Akaike T, Yoshida M, Goto S, Horie H, Maeda H. Potentiation of nitric oxide-mediated vasorelaxation by xanthine oxidase inhibitors. *Proc Soc Exp Biol Med*. 1996;21:366–373.
- Grunfeld S, Hamilton CA, Mesaros S, McClain SW, Dominiczak AF, Bohr DF, Malinski T. Role of superoxide in the depressed nitric oxide production by the endothelium of genetically hypertensive rats. *Hypertension*. 1995;37:854–857.
- Tschudi M, Mesaros S, Lüscher TF, Malinski T. Direct in situ measurement of nitric oxide in mesenteric arteries. *Hypertension*. 1996;27:32–35.
- Schnackenberg CG, Welch WJ, Wilcox CS. Normalization of blood pressure and renal vascular resistance in SHR with a membrane-permeable superoxide dismutase mimetic: role of nitric oxide. *Hypertension*. 1998;32:59–64.
- Li PF, Dietz R, von Harsdorf R. Differential effect of hydrogen peroxide and superoxide anion on apoptosis and proliferation of vascular smooth muscle cells. *Circulation*. 1997;96:3602–3609.
- Zafari AM, Ushio-Fukai M, Akers M, Yin Q, Shah A, Harrison DG, Taylor WR, Griendling KK. Role of NADH/NADPH oxidase-derived  $\text{H}_2\text{O}_2$  in angiotensin II-induced vascular hypertrophy. *Hypertension*. 1998;32:488–495.
- Mohazzab KM, Kaminski PM, Wolin MS. NADH oxidoreductase is a major source of superoxide anion in bovine coronary artery endothelium. *Am J Physiol*. 1994;266:H2568–H2572.
- Pagano P, Ito Y, Tornheim K, Gallop P, Tauber A, Cohen R. An NADPH oxidase superoxide-generating system in the rabbit aorta. *Am J Physiol*. 1995;268:H2274–H2280.
- Jones SA, O'Donnell VB, Wood JD, Broughton JP, Hugher EJ, Jones OT. Expression of phagocyte NADPH oxidase components in human endothelial cells. *Am J Physiol*. 1996;271:H1626–H1634.
- Ushio-Fukai M, Zafari AM, Fukui T, Ishizaka N, Griendling KK. *p22phox* is a critical component of the superoxide-generating NADH/NADPH oxidase system and regulates angiotensin II-induced hypertrophy in vascular smooth muscle cells. *J Biol Chem*. 1996;271:23317–23321.
- Rajagopalan S, Kurz S, Münzel T, Tarpey M, Freeman BA, Griendling KK, Harrison DG. Angiotensin II-mediated hypertension in the rat increases vascular superoxide production via membrane NADH/NADPH oxidase activation: contribution to alterations of vasomotor tone. *J Clin Invest*. 1996;97:1916–1923.
- Bradford MM. A rapid and sensitive method for the quantification of microgram quantities of protein utilizing the principle of protein-dye binding. *Anal Biochem*. 1976;72:248–254.
- Gilliland G, Perrin S, Blanchard K, Bunn HF. Analysis of cytokine mRNA and DNA: detection and quantitation by competitive polymerase chain reaction. *Proc Natl Acad Sci U S A*. 1990;87:2725–2729.
- Fukui T, Lassège B, Kai H, Alexander RW, Griendling KK. Cytochrome b-558  $\alpha$ -subunit cloning and expression in rat aortic smooth muscle cells. *Biochim Biophys Acta*. 1995;1231:215–219.
- Fortuño MA, Ravassa S, Etayo JC, Díez J. Overexpression of Bax protein and enhanced apoptosis in the left ventricle of spontaneously hypertensive rats: effects of AT<sub>1</sub> blockade with losartan. *Hypertension*. 1998;32:280–286.
- van Gorp AW, van Ingen Schenau DS, Hoeks APG, Struijker Boudier HAJ, Reneman RS, De Mey JGR. Aortic wall properties in normotensive and hypertensive rats of various ages in vivo. *Hypertension*. 1995;26:363–368.
- Lee RM, Forrest JB, Garfield RE, Daniel EE. Comparison of blood vessel wall dimensions in normotensive and hypertensive rats by histometric and morphometric analysis. *Blood Vessels*. 1983;20:245–254.
- Dijkstra CD, Döpp EA, Joling P, Kraal G. The heterogeneity of mononuclear phagocytes in lymphoid organs: distinct macrophage subpopulations in the rat recognized by monoclonal antibodies ED1, ED2 and ED3. *Immunology*. 1985;54:589–599.
- Liochev SI, Fridovich I. Lucigenin (bis-N-methylacridinium) as a mediator of superoxide anion production. *Arch Biochem Biophys*. 1997;337:115–120.
- Li Y, Zhu H, Kuppasamy P, Roubaud V, Zweier JL, Trush MA. Validation of lucigenin (bis-N-methylacridinium) as a chemiluminescent probe

- for detecting superoxide anion radical production by enzymatic and cellular systems. *J Biol Chem*. 1998;273:2015–2023.
27. Griendling KK, Minieri CA, Ollerenshaw JD, Alexander RW. Angiotensin II stimulates NADH and NADPH oxidase activity in cultured vascular smooth muscle cells. *Circ Res*. 1994;74:1141–1148.
  28. Meier B, Radeke HH, Selle S, Younes M, Sies H, Resch K, Habhermehl GG. Human fibroblasts release reactive oxygen species in response to interleukin-1 or tumor necrosis factor- $\alpha$ . *Biochem J*. 1989;263:539–545.
  29. Dinanuer MC, Orkin SH, Brown R, Jesaitis AJ, Parkos CA. The glycoprotein encoded by the X-linked chronic granulomatous disease locus is a component of the neutrophil cytochrome b complex. *Nature*. 1987;327:717–720.
  30. Clozel M, Kuhn H, Hefti F, Baumgartner HR. Endothelial dysfunction and subendothelial monocyte macrophages in hypertension: effect of angiotensin converting enzyme inhibition. *Hypertension*. 1991;18:132–141.
  31. Fukui T, Ishizaka N, Rajagopalan S, Laursen JB, Capers Q, Taylor WR, Harrison DG, de Leon H, Wilson JN, Griendling KK. p22phox mRNA expression and NADPH oxidase activity are increased in aortas from hypertensive rats. *Circ Res*. 1997;80:45–51.
  32. Mizuno K, Tani M, Nimura S, Fukuchis S. Effect of delapril on the vascular angiotensin II release in isolated hind legs of the spontaneously hypertensive rat: evidence for potential relevance of vascular angiotensin II to the maintenance of hypertension. *Clin Exp Pharmacol Physiol*. 1991;18:619–625.
  33. Otsuka S, Sugano M, Makino N, Sawada S, Hata T, Niho Y. Interaction of mRNAs for angiotensin II type 1 and type 2 receptors to vascular remodeling in spontaneously hypertensive rats. *Hypertension*. 1998;32:467–472.
  34. Grima M, Welsch C, Giesen-Crouse EM, Coquard C, Barthelmebs M, Imbs JL. Age-related variations in tissue angiotensin converting enzyme activities: comparison between spontaneously hypertensive and Wistar-Kyoto rats. *J Hypertens*. 1990;8:697–702.
  35. Beckman JS, Beckman TW, Chen J, Marshall PA, Freeman BA. Apparent hydroxyl radical production by peroxynitrite: implications for endothelial injury from nitric oxide and superoxide. *Proc Natl Acad Sci U S A*. 1990;87:1620–1624.
  36. Bauerbasch J, Bouloumié A, Mülsch A, Wiemer G, Fleming I, Busse R. Vasodilator dysfunction in aged spontaneously hypertensive rats: changes in NO synthase III and soluble guanylyl cyclase expression, and in superoxide anion production. *Cardiovasc Res*. 1998;37:772–779.
  37. Kojda G, Kottenberg K, Hacker A, Noack E. Alterations of the vascular and the myocardial guanylate cyclase/cGMP-system induced by long-term hypertension in rats. *Pharm Acta Helv*. 1998;73:27–35.
  38. Sagar S, Kallo J, Kaul N, Ganguly NK, Sharma BK. Oxygen free radicals in essential hypertension. *Mol Cell Biochem*. 1992;111:103–108.
  39. Mehta JL, Lopez LM, Chen L, Cox OE. Alterations in nitric oxide synthase activity, superoxide anion generation, and platelet aggregation in systemic hypertension, and effects of celiprolol. *Am J Cardiol*. 1994;74:901–905.